

# EFFECT OF WATER DENSITY INVERSION ON THE PLANE-PARALLEL FLOW AND HEAT TRANSFER IN A CHANNEL OF CONSTANT WIDTH

I. M. Galiev and P. T. Zubkov

UDC 532.529.2:536.421

The results of a numerical study of the effect of cold-water density inversion (Prandtl number  $Pr=11.59$ ) on the flow and heat transfer in a horizontal plane-parallel channel with isothermal top and bottom walls are presented. The calculations were performed for the Grashof number  $Gr=3 \cdot 10^4$ , the Reynolds number  $Re=10$ , and the channel segment length-to-height ratio  $l/d=40$ . The wall temperature was so varied that the temperature difference between the top and bottom walls remained constant.

A specific feature of the problem in question is the presence of the simultaneous forced and natural convection, i.e. mixed convection. The first studies of mixed convection considered only fully developed flows [1, 2]. However, in many cases, for instance, in heat exchangers, the channel is too short to ensure developed flow and, hence, information on the flow and heat transfer characteristics in the entrance region is also important [3–7]. The thermal instability associated with convection between two heated plates results in the appearance of secondary flows and a noticeable enhancement of the heat transfer.

As a rule, secondary channel flows take the form of lengthwise rolls [8]. However, at small Reynolds numbers ( $Re \sim 10$ ) the minimum critical Rayleigh (or Grashof) numbers corresponding to disturbances in the form of rolls with axes directed parallel and normal to the flow are very close to each other [9]. This is why, for fairly intense natural convection, flows directed opposite to those in forced convection may develop [10, 11].

Neglecting longitudinal disturbances, we can use the two-dimensional formulation of the plane-parallel channel flow equations. To confirm this assumption, we performed additional three-dimensional calculations for the flow in a channel with the dimensions (height:width:length) 1:10:16 on a 15:50:200 grid. The results for the middle of the channel agreed very well with the results for the two-dimensional problem on a similar grid (height-to-length ratio 1:16 and a 15:200 grid). It follows that, at least in the initial section of the channel, the use of the two-dimensional model is justified.

Most studies of mixed convection in pipes deal with fluids whose thermal expansion coefficient is constant. However, near the freezing point the assumption of constancy of the thermal expansion coefficient is not valid since the density of water has a maximum near  $4^\circ\text{C}$ . The heat transfer in cold-water forced convection was studied not only for its a theoretical interest but also because it might have engineering applications and could help to explain some natural phenomena [12].

## 1. FORMULATION OF THE PROBLEM

Consider a flow of viscous incompressible heat-conducting fluid in a plane channel with parallel walls of length  $l$  and width  $d$ . The temperature of the walls is constant, the bottom wall being warmer. At the channel entrance, the fluid temperature is equal to  $4^\circ\text{C}$  and the velocity is constant across the section. On the channel walls, the fluid velocity is zero. For investigating mixed convection, we write the system of incompressible-fluid equations in the Boussinesq approximation in the following nondimensional form:

$$\begin{aligned}
 \partial U / \partial Fo + U \partial U / \partial X + V \partial U / \partial Y &= -\partial P / \partial X + (1/Re) \Delta U \\
 \partial V / \partial Fo + U \partial V / \partial X + V \partial V / \partial Y &= -\partial P / \partial Y + (1/Re) \Delta V + (Gr/Re^2) |\theta|^\gamma \\
 \partial U / \partial X + \partial V / \partial Y &= 0, \quad \partial \theta / \partial Fo + U \partial \theta / \partial X + V \partial \theta / \partial Y = 1/(Re Pr) \Delta \theta \\
 X = x/d, \quad Y = y/d, \quad U = u/u_e, \quad V = v/u_e \\
 \theta = (T - T_i)/(T_d - T_u), \quad Fo = t/(d/u_e), \quad P = p/(\rho u_e^2) \\
 Re = (u_e d)/\nu, \quad Pr = \nu/\alpha, \quad Gr = (g \beta |T_d - T_u|^\gamma d^3)/\nu^2
 \end{aligned}
 \tag{1.1}$$

Surgut. Translated from *Izvestiya Rossiiskoi Akademii Nauk, Mekhanika Zhidkosti i Gaza*, No. 1, pp. 72–78, January–February, 2000. Original article submitted October 27, 1998.

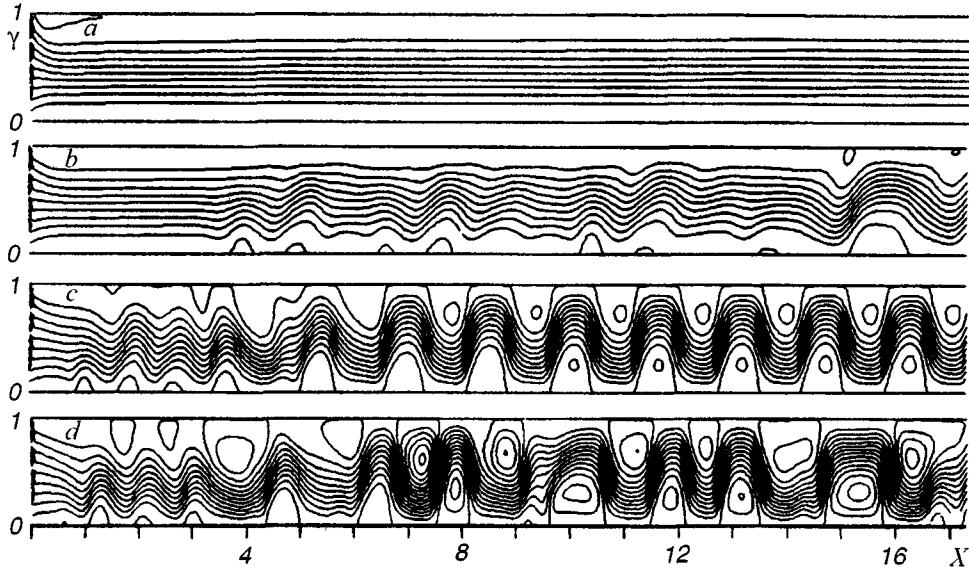


Fig. 1. Stream functions for different wall temperatures:  $\theta_d=0, 0.5, 0.85,$  and  $1$  (a–d).

Here,  $Re$ ,  $Pr$ , and  $Gr$  are the Reynolds, Prandtl, and Grashof numbers, respectively.

The dependence of the water density  $\rho$  on the temperature  $T$  is taken in the form suggested by Gebhart and Mollendorf [13]:

$$\rho = \rho_i (1 - \beta |T - T_i|^\gamma)$$

Here,  $\rho_i$  is the water density at  $4^\circ\text{C}$ ,  $\beta = 9.297173 \cdot 10^{-6} \text{ K}^{-\gamma}$ , and  $T_i$  equal to  $4^\circ\text{C}$  is the density inversion point.

In nondimensionalizing, distance was scaled to  $d$ , time to  $d/u_e$ , velocity to  $u_e$ , pressure to  $\rho u_e^2$ , and temperature to  $T_d - T_u$ ; here,  $T_d$  and  $T_u$  are the temperatures of the top and bottom walls, and  $u_e$  is the longitudinal velocity component at the channel entrance.

Equations (1.1) were solved for the following boundary conditions:

$$\begin{aligned} Fe=0, \quad X=0: \quad V=0, \quad U=1, \quad \theta=0 \\ 0 \leq X \leq L, \quad Y=1, \quad Y=0: \quad U=V=0 \\ L < X \leq L + L_1, \quad Y=0, \quad Y=1: \quad U=V=\partial\theta/\partial Y=0 \\ X=L + L_1: \quad \partial U/\partial X = \partial V/\partial X = \partial\theta/\partial X = 0 \end{aligned} \quad (1.2)$$

The nondimensional temperatures of the bottom and top walls were varied from 0 to 1 and from  $-1$  to 0, respectively:

$$0 \leq X \leq L, \quad Y=0: \quad \theta_d = 0 \dots 1, \quad Y=1: \quad \theta_u = \theta_d - 1 \quad (1.3)$$

In order to specify the exit boundary conditions (1.2) at  $X=L + L_1$ , we assume that, near the exit, there is a channel segment of length  $L_1$  with adiabatic walls, which ensures the regression of the influence of natural convection. In this study, the length of this segment ( $L_1=20$ ), derived from the test calculations, was sufficient for flow stabilization.

The local Nusselt number and the friction coefficient on the channel walls are defined as follows:

$$Nu = hd/k = -\partial\theta/\partial Y, \quad f = \pm 2\sigma / (\rho u_e^2) = \pm (2/Re)(\partial U/\partial Y)$$

Here,  $h$  is the heat transfer coefficient,  $k$  is the thermal conductivity, and  $\sigma$  is the stress.

The two-dimensional problem of water channel flow was solved numerically using the control-volume method and the SIMPLER algorithm on a uniform grid with 23 control volumes over the channel height [14]. This grid was sufficient for a qualitative description of the flow and heat transfer.

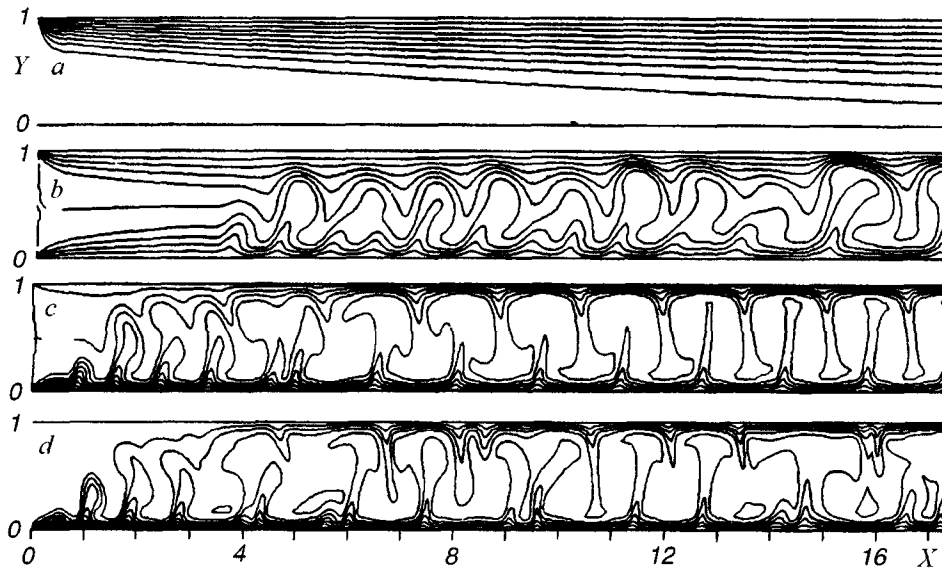


Fig. 2. Temperature fields for different wall temperatures:  $\theta_d=0, 0.5, 0.85,$  and  $1$  (a-d).

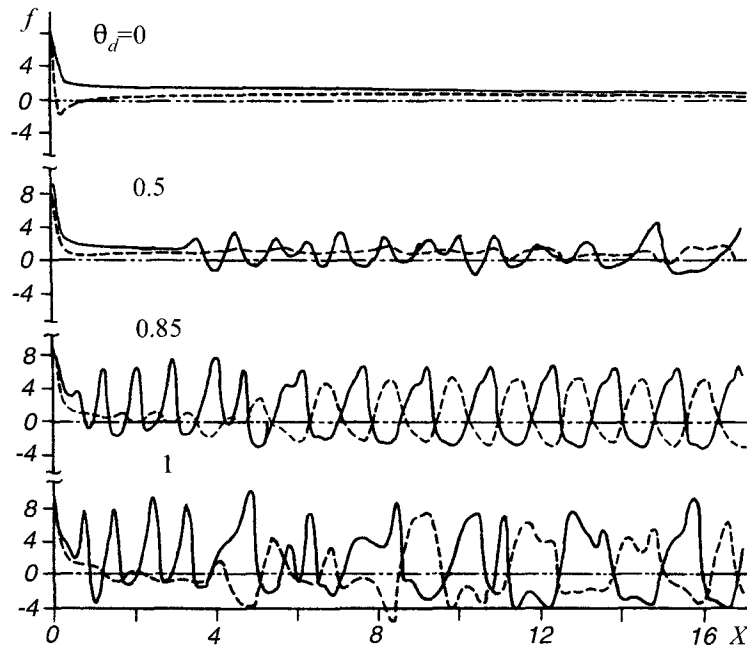


Fig. 3. Friction coefficients at the top (broken curve) and bottom (continuous curve) walls for different wall temperatures.

## 2. RESULTS AND DISCUSSION

The chosen Grashof number  $Gr=3 \cdot 10^4$  was not too large but, at the same time, it made it possible to obtain essentially different kinds of flow within the problem formulation considered. In our numerical experiments, in accordance with boundary condition (1.3), the wall temperature was varied in such a way that the difference between the temperatures of the walls remained constant. Accordingly, in what follows we will use the bottom wall temperature  $\theta_d$  as the variable. Examples of flow patterns and temperature fields are given in Figs. 1 and 2.

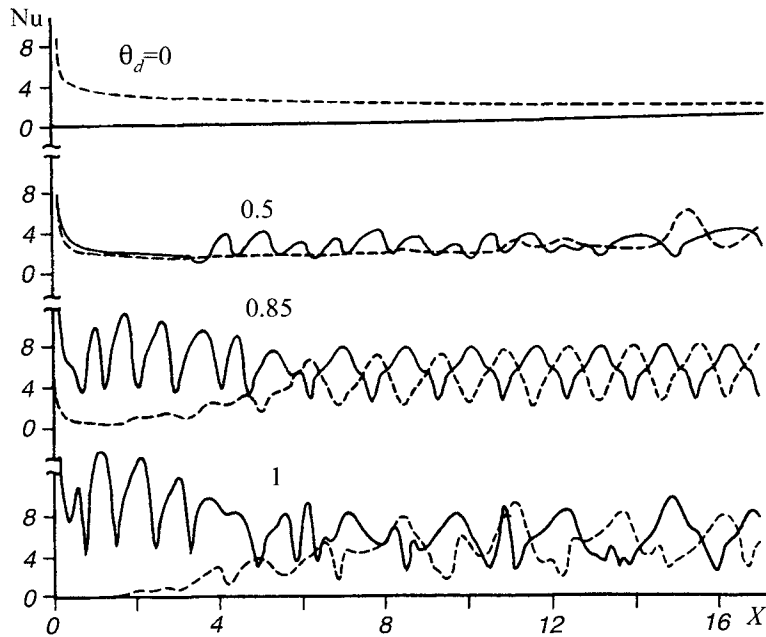


Fig. 4. Nusselt numbers at the top (broken curve) and bottom (continuous curve) walls for different wall temperatures.

For  $\theta_w=0$ , in the entrance region of the heated segment, near the top wall a reverse flow develops. This disappears downstream and the flow becomes parabolic. As the bottom wall temperature increases, the reverse flow becomes weaker and disappears completely at  $\theta_w=0.35$ . With further increase in  $\theta_w$ , at a certain distance from the channel entrance there appears a secondary flow with an upward motion of the fluid near the bottom wall. In the middle of the channel, this warm stream meets the colder main stream. The main flow, which has a parabolic profile at the heated region entrance, is narrowed by the rising streams. As a result, the flow and the temperature field are almost unchanged near the top wall despite the fact that, near the bottom wall, both the velocity and temperature fields oscillate almost periodically and even form small local reverse-flow regions. These regions can be clearly seen in Fig. 3. When the longitudinal velocity component near the wall is negative, the friction coefficient takes negative values.

A further increase in  $\theta_w$  results in the appearance of a secondary flow near the top wall and intensifies the secondary flow near the bottom wall. Figures 1 and 2 show an example of this flow and the temperature field for  $\theta_w=0.5$ . At a distance of approximately  $X \approx 3.5$  from the channel entrance, a reverse flow develops near the bottom wall. Downstream, the rising of warm fluid from the bottom wall and the sinking of cold fluid from the central region oscillate, with the bottom half of the channel being mainly involved. Then, at a distance of approximately  $X \approx 13$  from the channel entrance, a secondary flow near the top wall appears, producing a change in the flow and temperature field structure. Beyond this transition region, the flow becomes almost periodic and the friction coefficient amplitude increases, i. e. the reverse flow becomes more intense.

With increase in  $\theta_w$ , the coordinate of secondary flow onset and the transition region are displaced towards the channel entrance. The flow structure and the temperature field become strictly periodic, as is clear from Figs. 1 and 2 for  $\theta_w=0.85$ , and the intensities of the secondary flows near the top and bottom walls are almost identical (Fig. 3). A further increase in  $\theta_w$  results in the breakdown of the flow periodicity, as may be seen in Figs. 1, 2, and 3 for  $\theta_w=1$ .

Observations of the heat transfer variation during the passage from  $\theta_w=0$  to  $\theta_w=1$  reveal the following pattern. When no secondary flow exists, the heat transfer is associated with the thermal conductivity of the fluid. On the range between  $\theta_w=0$  and  $\theta_w=0.4$ , the local Nusselt number at the top wall is greater than that at the bottom wall. This is because the temperature of the water entering the channel is zero ( $\theta_c=0$ ). When  $\theta_w=0.4$ , the secondary flow near the bottom wall induces heat flux oscillations while, at the top wall, the heat flux is constant.

A further increase in  $\theta_w$  results in the earlier appearance of the heat flux oscillations on the bottom wall, and downstream, when the secondary flow appears at the top wall, the Nusselt number  $Nu$  at the top wall also oscillates, as is clear from Fig. 4 for  $\theta_w=0.5$  and  $0.85$ . For  $\theta_w=0.85$ , at the channel entrance the heat fluxes at the top and bottom differ substantially. This is associated with the difference in the secondary flow intensities at the top and bottom walls. Near the bottom wall, a secondary flow starts to develop in the form of rising warm fluid which is then carried downstream by the

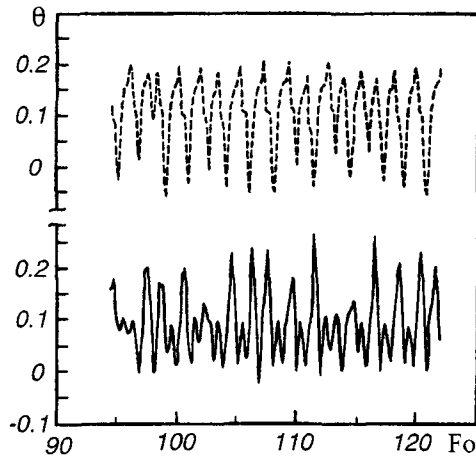


Fig. 5

Fig. 5. Temperature variation at different points for  $\theta_w=0.5$ ,  $Y=0.5$ :  $X=35$  (broken curve) and  $X=14$  (continuous curve).

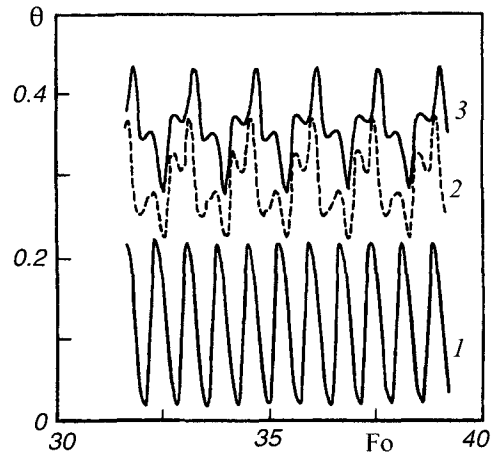


Fig. 6

Fig. 6. Temperature variation at the points  $Y=0.5$ ,  $X=2$ ,  $6$ , and  $20$  (curves 1-3) for  $\theta_w=0.85$ .

main flow, so that only after traveling a certain distance does the warm fluid reach the top flow layers. With increase in  $\theta_w$ , the amplitude of variation of  $Nu$  increases and, for fairly large  $\theta_w$ , the variation of  $Nu$  becomes chaotic, as is clear from Fig. 4 for  $\theta_w=1$ .

We will now consider the channel flow temperature oscillations with time. Increasing  $\theta_w$  from 0 to 1 leads first to the appearance of an almost periodic secondary flow ( $X=35$ ,  $Y=0.5$ ) which, with further increase in  $\theta_w$ , becomes more and more nearly periodic. With further increase in  $\theta_w$ , the periodic flow changes its structure and, near the top wall, a reverse flow arises. For  $\theta_w=0.5$ , up to the coordinate  $X\approx 13$  the flow is strictly time-periodic. In the region  $X=13-16$ , when the flow structure changes, as is clear from Fig. 5 the flow is almost chaotic, while beyond  $X=16$  it becomes almost periodic (Fig. 5).

With further increase in  $\theta_w$ , the flow becomes periodic over the whole channel. For  $\theta_w=0.85$ , this is illustrated in Fig. 6. Then, the flow becomes chaotic, but in the entrance region it remains periodic.

Thus, due to the water density maximum at  $4^\circ\text{C}$ , for the same Grashof number we observed several different kinds of flow.

*Summary.* The effect of water density inversion in a plane-parallel channel flow with isothermal walls and an entrance water temperature equal to that at the density inversion point is investigated. It is shown that for different wall temperatures but the same difference between the top and bottom walls several qualitatively different kinds of flow are possible. These may be briefly characterized as follows: parabolic flow, a weak almost periodic flow near the bottom wall, a flow periodic in the entrance region near the bottom wall and almost periodic downstream near the top wall, a periodic flow with large reverse-flow regions, and a chaotic flow. With the successive realization of these kinds of flow, the reverse-flow intensity and the amplitude of the Nusselt number variation increase, which, in a sense, is equivalent to an increase in the Grashof number.

## REFERENCES

1. S. Ostrach and Y. Kamotani, "Heat transfer augmentation in laminar fully developed channel flow by means of heating from below." *Trans. ASME, J. Heat Transfer*, **97**, No. 2, 220 (1975).
2. K.-C. Chiu, J. Ouazzani, and F. Rosenberger, "Mixed convection between horizontal plates. II. Fully developed flow," *Intern. J. Heat Mass Transfer*, **30**, No. 8, 1655 (1987).
3. Y. Kamotani and S. Ostrach, "Effect of thermal instability on thermally developing laminar channel flow," *Trans. ASME, J. Heat Transfer*, **98**, No. 1, 62 (1976).
4. F. P. Incropera and J. A. Schutt, "Numerical simulation of laminar mixed convection in the entrance region of horizontal rectangular ducts," *Numer. Heat Transfer*, **8**, No. 6, 707 (1985).
5. K.-C. Chiu and F. Rosenberger, "Mixed convection between horizontal plates. I. Entrance effects," *Intern. J. Heat Mass Transfer*, **30**, No. 8, 1645 (1987).
6. J. R. Maughan and F. P. Incropera, "Secondary flow in horizontal channels heated from below." *Experim. Fluids*, **5**, No. 5, 334 (1987).

7. J. R. Maughan and F. P. Incropera, "Regions of heat transfer enhancement for laminar mixed convection in a parallel plate channel," *Intern. J. Heat Mass Transfer*, **33**, No. 3, 555 (1990).
8. A. V. Kuz'minskii and E. M. Smirnov, "Experimental study of instabilities in the flow in a long square channel rotating about a transverse axis," *Izv. Ross. Akad. Nauk, Mekh. Zhidk. Gaza*, No. 2, 87 (1996).
9. G. Z. Gershuni and E. M. Zhukhovitskii, *Convective Stability in an Incompressible Fluid* [in Russian], Nauka, Moscow (1972).
10. G. Evans and R. Greif, "Buoyant instabilities in downward flow in a symmetrically heated vertical channel," *Intern. J. Heat Mass Transfer*, **40**, No. 10, 2419 (1997).
11. I. M. Galiev and P. T. Zubkov, "Plane convective water flow in a horizontal channel," *RNKT-2. V.3* [in Russian], Moscow (1998), pp. 54–57.
12. G. J. Hwang and C. W. Tsai, "Theoretical and experimental studies of laminar mixed convection in water pipe flow with density inversion effect," *Intern. J. Heat Mass Transfer*, **40**, No. 9, 2019 (1997).
13. B. Gebhart and J. Mollendorf, "A new density relation for pure and saline water," *Deep Sea Res.*, **24**, No. 9, 831 (1977).
14. S. Patankar, *Numerical Heat and Fluid Flow*, McGraw Hill, New York (1984).